

INFRARED THERMAL IMAGING AND POLLUTANT EMISSIONS OF ULTRA-LEAN TURBULENT PRODUCER GAS FLAME

M. Z. Qureshi*, **C. Caligiuri***, **M. Renzi***, **V. Benedetti***, **F. Patuzzi***,
M. Baratieri*

MQureshi@unibz.it

*Faculty of Engineering, Free University of Bolzano, piazza Università 1, 39100, Italy

Abstract

This work aims at supplying some fundamental insights of producer gas combustion and it is developed in the framework of the Green Deal project FRONTSHIP. To this aim, an in-house designed combustion chamber is directly coupled with a fluidized bed gasifier operated with wood packaging waste (e.g., disused pallets). Stable combustion process of producer gas mixtures, also at very-lean equivalence ratio (ER), is achieved and presented as an interesting insight against rising clean energy demand of industrial users with net-zero emissions. Thermal imaging based IR thermography technique is employed and time resolved flame images were viewed for flame temperature field and topology analysis at ER, $\Phi \sim 0.20 - 0.85$. The producer gas flame was quite stable and evenly distributed in the combustion chamber volume at ER = 0.85. Conversely, at lower ER, $\Phi = 0.20, 0.43$, the producer gas flame was strongly unstable due to several competing factors related to fluid dynamics and chemical kinetics. Finally, the re-stabilization opportunity of producer gas flame was revealed with the addition of a small share of methane gas ($\sim 5\%$ CH₄) at ER, $\Phi \sim 0.20 - 0.25$, which could represent a possible solution to achieve flame stability at ultra-lean combustion. Moreover, CO concentrations of 53 ppm and NO_x emissions of 33 ppm were produced mainly due to fuel-prompt mechanism during ultra-lean combustion of producer gas mixture (G1) 3.70 % CH₄, 18.16 % H₂, 8.69 % CO₂, 21.79 % CO, 7.26 % H₂O, and 40.40 % N₂.

Introduction

The use of clean fuels for thermal energy production still presents several challenges, especially when low Lower Heating Value (LHV) fuels are adopted. Among such fuels, producer gas from biomass and wood wastes gasification represents an interesting low-environmental impact solution to decarbonize high-temperature industrial processes. However, stable and clean combustion of such fuels still need to be investigated in depth. To acquire deep insights into flame instability driving events, the measurement of flame temperature with fast temporal response can be adopted. The use of thermocouples as probing method is a low cost and simple solution, but it does not have a proper response to fast phenomena and could disturb fluid dynamics of the medium. Especially, the thin wire thermocouples are used and

give support to validate kinetic modelling and develop advance non-intrusive techniques for detecting flame temperature. At certain flame temperatures, soot particles and gas molecules emit strong thermal radiations lying in the spectral regions of IR (900 nm – 14000 nm) and VIS range (400 nm – 900 nm), respectively. Magnitude of radiation intensity and underlying spectrum, depending on combustion state, might serve as basis in the development of diagnostic and monitoring tools. For example, detection of black body emissions serves in the development of radiation thermometry and thermography techniques. In recent years, several thermographic studies have been conducted on open pool fires or flames. For example, Sudheer et al. [1] studied open fired gasoline flames; authors inferred flame emissivity mathematically from mass burning rate analysis and compared with experimental emissivity from thermal camera in the spectral range (7.5 – 14 μ m). Raj et al. [2] characterized turbulent diffusion flames of gasoline and diesel pool fires of various diameters theoretically and experimentally with IR camera by proposing refine methods. Loboda et al. presented the spectrographic work with reference to black body spectrum and explained the radiation spectra to explore combustion of various vegetation materials, liquid fuels (alcohol, diesel, gasoline), woods and coal. In this work, the optical-based flame imaging technique has been developed for the first time for temperature field and flame topology observations of a confined producer gas flames at lean conditions in a combustion chamber.

Methods

In this work, IR flame imaging technique has been developed for measuring flame temperature field with three biomass-derived green producer gas mixtures G0, G1 and G2 (see **Table 1**). For this purpose, an in-house designed, optically accessible combustion test-rig of upto 30 kW thermal power is operated as shown in Figure 1 (Right). Size of the combustion chamber is 820 mm \times 520 mm \times 520 mm while burner internal diameter is 68 mm.

Table 1. Producer gas compositions

Gas mixture(s)	Methan flow rate [m ³ /h]	CH ₄ [% vol.]	H ₂ [% vol.]	CO ₂ [% vol.]	CO [% vol.]	H ₂ O [% vol.]	N ₂ [% vol.]	LHV [MJ/m ³]
G0	0.00	1.90	18.50	8.85	22.20	7.40	41.15	5.48
G1	0.11	3.70	18.16	8.69	21.79	7.26	40.40	6.04
G2	0.22	4.64	17.98	8.60	21.58	7.19	40.00	6.33

The measurement of producer gas consumption rate is performed using FCI-ST80 thermal mass flow meter, installed on the spilled outlet pipe of the gasifier and signal is acquired using cDAQ NI-9203. Consumption rate of methane flow rate is controlled by Brooks-0254 mass flow controllers. Thermal imaging based IR thermography technique is employed using IR thermal Camera FLIR - A700 of spectral range 7.5 – 14 μm with 30 Hz acquisition frequency. The ZnSe thermal window is located on combustion chamber along the zx-plane and IR camera is placed close to the window facing towards the zx-plane; hence, flame is projected as a 2D image as shown in schematic **Figure 1 (Left)**. Intrusive measurements were also conducted using N type thin wire thermocouples to calibrate emissivity of flame to be utilized in post-processing of flame images. The flue gas emissions were also monitored.

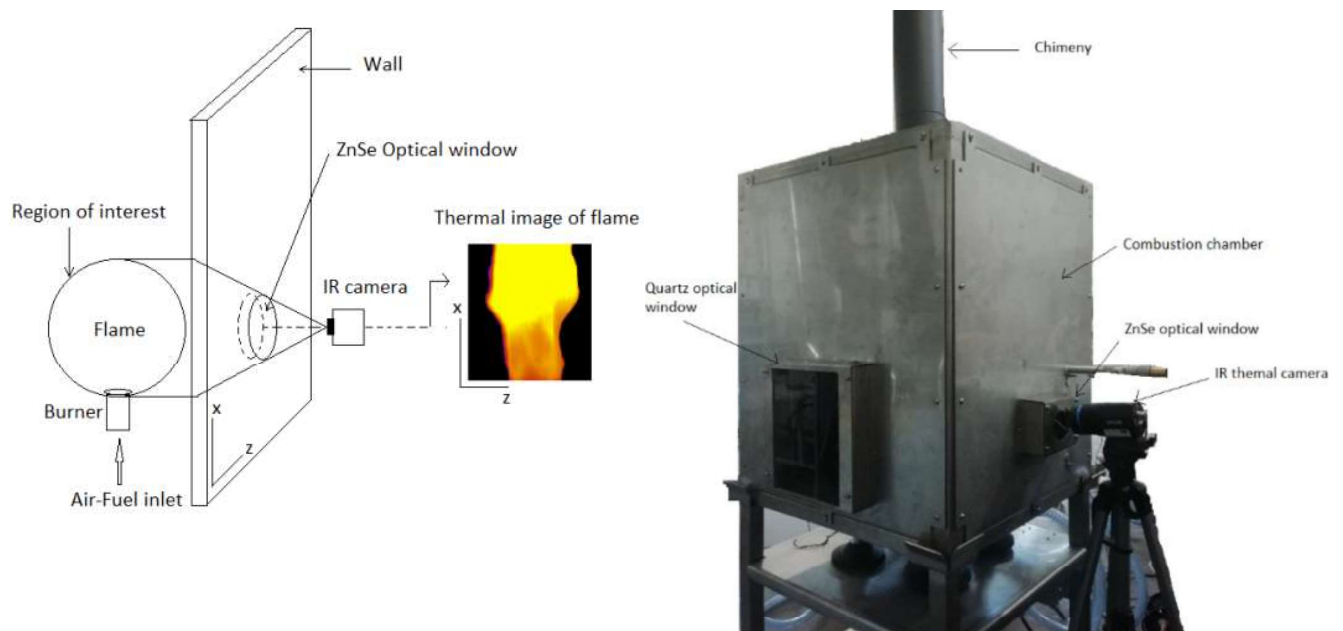


Figure 1. (Left) Schematic diagram of imaging technique. **(Right)** Combustion chamber with optical access

Flame image processing

FLIR thermal camera videos at different thermal loads and equivalence ratio points were recorded and images were processed in three major steps: (1) Emissivity of producer gas flame was corrected with maximum flame temperature measured by thermocouples; to this end, the range of emissivity values of 0.2 to 0.3 was set to match the measured range of temperature values of 900 °C - 1022 °C at lean $\Phi \sim 0.65 - 0.85$. (2) Pixel size 344 \times 357 of flame images was used and pre-processing methods were implemented for identifying the flame zone and its boundaries by applying an edge detection algorithm. To isolate the intense foreground flame from the background, the sobel operation and canny edge detection operation were applied to detect the edges (high gradient intensities in x and z direction) around the flame

boundary, as shown in **Figure 2 (a)**. These images were converted into a binary [0; 1] field in which the area inside the flame boundary represents white region [1], while the remaining (outer) region comprises black [0] region, as shown in **Figure 2 (b)**. In the next step, pixels data of flame region were substituted with color pixels data of FLIR image, as show in **Figure 2 (c)**.

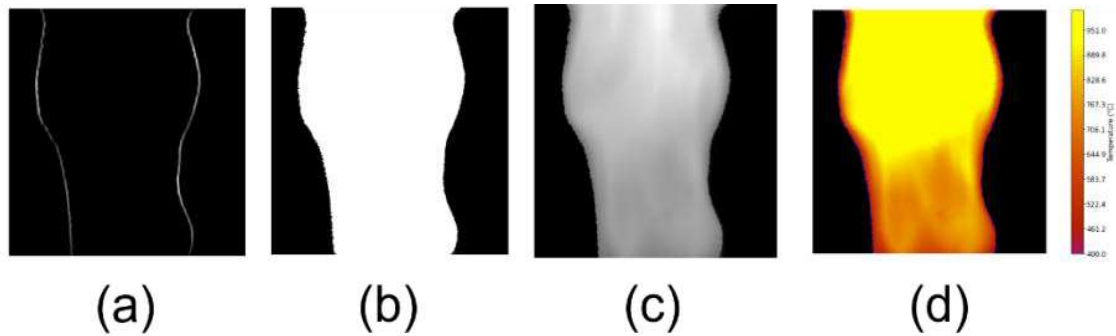


Figure 2. Flame image processing: Edge detection **(a)** Binary field **(b)** Pixel substitution **(c)** Corrected flame image **(d)**.

(3) These pre-processed RGB images were then converted into grey scale images. Using these grey and RGB scale pixel range, a mapping function was built to determine grey scale and thermal data at each pixel of images. A reference location was defined in the zx-plane according to a reference thermocouple coordinate (x, z) in the flame image (including thermocouples). A pixel based correlation factor was defined at that reference location using the grey scale and temperature value, using *Correlation factor = Measured temperature / Grey scale* was used to rescale and get the corresponding corrected flame temperature, see **Figure 2 (d)**.

Results: Flame visualizations and emissions

The experimental flame data was obtained from the experimental campaign using the described methodology to present flame temperature and flame topologies of G0, G1 and G2 producer gas mixtures. Flame images of producer gas compositions, were viewed at 28 kW, 14 kW and 10 kW Thermal Loads (TL) for detecting flame temperature filed and topology analysis at equivalence ratios (ER), $\Phi \sim 0.20 - 0.85$. It is important to mention that these thermographic images do not depict the exact reaction zone; however, they identify the transition of burned to unburned regions. It appeared that producer gas G0 flame was quite stable and evenly distributed in the combustion chamber volume at ER, $\Phi = 0.85$. Moreover, the instantaneous flame

images showed analogous flame shapes at consecutive frames, which demonstrated a stable combustion behavior of producer gas G0 as shown in **Figure 3 (Left)**. Conversely, the producer gas flame images that were imaged at lower ER conditions led to the different outcomes. For instance, at ER, $\Phi = 0.43$, the producer gas G0 flame shapes at consecutive frames were distinct, as shown in **Figure 3 (Center)**, due to several competing factors related to fluid dynamics and chemical kinetics. The decrement of flame temperature was noticed at lower ER conditions, which may cause the reactions to be slower and may weaken the role of chemical kinetics associated with producer gas combustion process. In addition, it appears that high flow rates of air, as compared to fuel, contributed to shred the vortical structures that

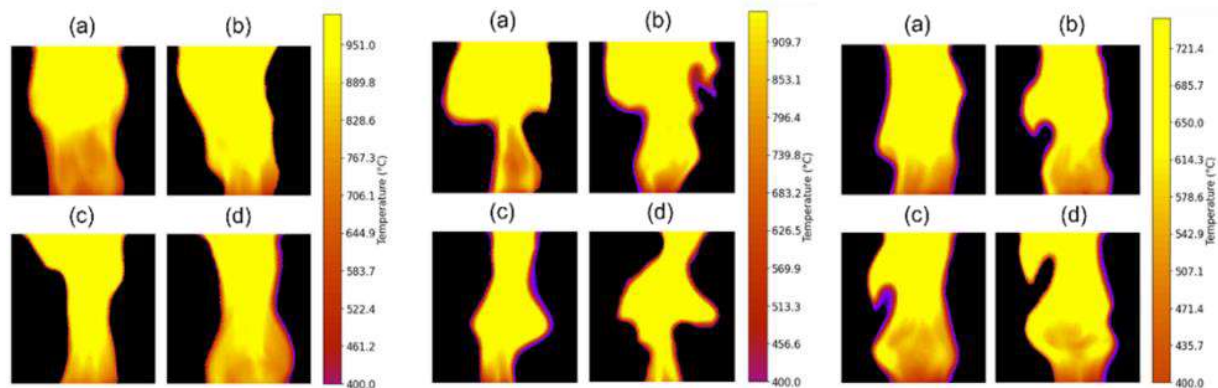


Figure 3. Time resolved flame thermal images of producer gas mixtures: G0, $\Phi = 0.85$ (Left), G0, $\Phi = 0.43$ (Center), G1, $\Phi = 0.25$ (Right)

perturbed the flame by creating the various branches on flame surfaces. Additionally, the phenomenon of flame neck thinning with uneven distribution was observed, which could be a sign of onset flame instability events. In particular, the flame surface area around flame neck was decreased as compared to flame at downstream location of combustion chamber. Moreover, the phenomenon of flame neck thinning became more evident when flame images were thermographically viewed at an ultra-lean ER, $\Phi \sim 0.20 - 0.25$. Nevertheless, it was observed that producer gas G0 flame was slightly uplifted due to flame destabilization and moved above the interrogation window. Finally, as shown in **Figure 3 (Right)**, the re-stabilization behavior of producer gas flame in G1 - G2 (only G1 mixture flame image is reported here) was revealed with the addition of a small share of methane gas (up to 5% CH₄) at ER, $\Phi = 0.20$, which could be a possible solution of producer gas flame instability at ultra-lean combustion process. This flame topology study has exhibited the flame instability events and occurrence of flame destabilization (close to blow off) events at very lean flame conditions. Moreover, the flue gas emissions O₂, CO, CO₂, and NO_x (NO and NO₂) were monitored at the outlet of the combustion chamber. In particular, CO concentrations of 9020 ppm were found to be at the highest level at ER, $\Phi = 0.85$, whereas, around 53 ppm were observed at very lean ER, $\Phi = 0.20$.

Following the same trend, NO_x emissions of 239 ppm concentration were observed at $\Phi = 0.85$ while the minimum concentration of 33 ppm at ER, $\Phi = 0.25$. These NO_x and CO pollutants were emitted mainly because of N₂ and CO components present in the fuel mixture.

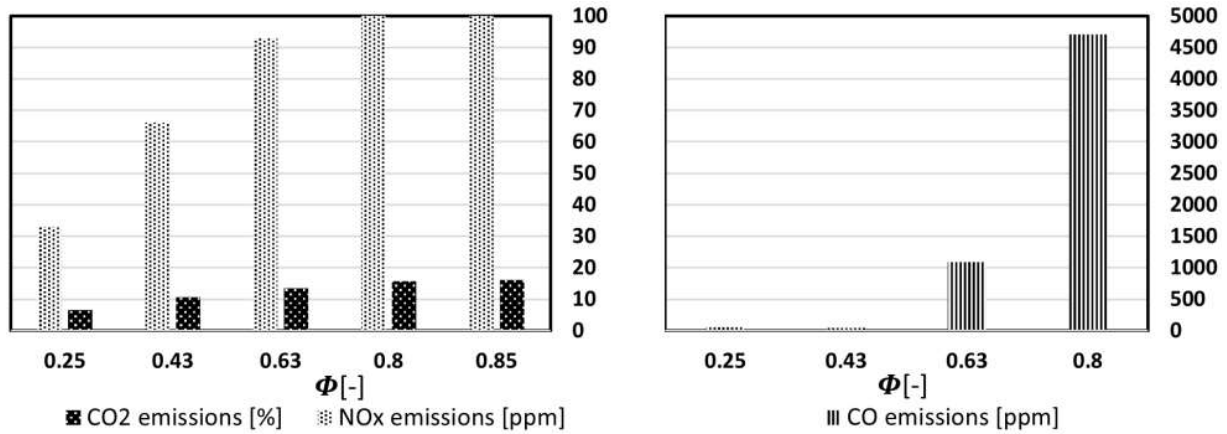


Figure 4. Flue gases: CO₂ and NO_x (Left) CO emissions (Right).

Conclusions

In this work, the combined impact of changing TL and lean ER conditions on the producer gas combustion parameters and flame topology are evaluated. Stable combustion operation of producer gas was observed at lean ER = 0.85 conditions; conversely, flame stability concerns at ultra-lean ER, $\Phi = 0.2$, were encountered. It was revealed that a small share of methane could be a viable solution to overcome producer gas flame instability issues in these conditions. It was concluded that low NO_x emissions ~ 35 ppm were produced mainly due to the fuel-prompt NO_x mechanism in G1 producer gas flame at ultra-lean combustion.

References

- [1] S. Sudheer and S. V. Prabhu, "Measurement of flame emissivity of gasoline pool fires," *Nucl. Eng. Des.*, vol. 240, no. 10, pp. 3474–3480, 2010, doi: 10.1016/j.nucengdes.2010.04.043.
- [2] V. C. Raj and S. V. Prabhu, "A refined methodology to determine the spatial and temporal variation in the emissivity of diffusion flames," *Int. J. Therm. Sci.*, vol. 115, pp. 89–103, 2017, doi: 10.1016/j.ijthermalsci.2017.01.016.